

Integrated taxonomy of three new species of *Glyphiulus* Gervais, 1847 (Diplopoda, Spirostreptida, Cambalopsidae) from Laos

Natdanai Likhitrakarn¹, Ekgachai Jeratthitikul², Parin Jirapatrasilp³ & Thomas Wesener^{4*}

Abstract. Three new species of the millipede genus *Glyphiulus* Gervais, 1847 are described and illustrated based on specimens collected from caves in Laos, namely *G. pseudocostulifer*, new species, from Oudomxay Province, *G. steineri*, new species, from Khammouan Province, and *G. houaphanhensis*, new species, from Houaphan Province. All of them belong to the *javanicus*-group, which share the unique structure of the first pair of legs in males and the carinotaxic formula of midbody rings. However, they differ from each other in the number of ommatidia, body colouration, the carinotaxic formula of the collum, as well as anterior and posterior gonopod structures. Mitochondrial COI sequences were used as DNA barcodes for species delineation, and were successfully obtained for two of the new species (*G. pseudocostulifer*, new species, and *G. steineri*, new species). Phylogenetic analyses revealed strong support for all examined *Glyphiulus* species, even for a pair of species which exhibited high morphological similarity, with mean uncorrected COI p-distances between *Glyphiulus* species ranging from 15–22%. Two additional *Glyphiulus* species are listed, but not described, as male material is lacking. One of them occurs in direct sympatry with *G. houaphanhensis*, new species. An identification key to the species of *Glyphiulus* so far recorded from Laos and a distribution map are also presented.

Key words. millipedes, key to species, cave fauna, molecular systematics, COI

INTRODUCTION

Laos, officially known as the Lao People's Democratic Republic, is a landlocked country in Southeast Asia. The majority of the country is traversed by the mighty Mekong River, which travels through rugged mountains and dense forests. The high biodiversity of the Greater Mekong region has resulted in the discovery of more than 3,000 new species over the past two decades, including numerous endemic species found nowhere else (WWF, 2021). In the past few years, the number of millipede species in Laos has rapidly and consistently increased. Since the most recent catalogue of the Diplopoda of Laos in 2014, which listed 34 species (Likhitrakarn et al., 2014), another 49 new species of millipedes have been discovered (Jiang et al., 2017; Likhitrakarn et al., 2017; Golovatch, 2018, 2019; Golovatch

& VandenSpiegel, 2017; Wesener, 2019; Nguyen et al., 2023; Srisonchai et al., 2023; Wesener et al., 2023). Evidently, there are numerous undiscovered millipede species in the country, eagerly anticipating our perseverance to discover them.

The millipede genus *Glyphiulus* Gervais, 1847 belongs to the family Cambalopsidae and has its primary habitat in Southeast Asia. Currently, there is a total of 76 recognised species of *Glyphiulus* distributed in East and Southeast Asian countries: 51 of which have been recorded in China, nine species in Vietnam, seven species in Thailand, six species in Laos, and one species each in Japan, Cambodia, and Indonesia (more specifically, Java) (Likhitrakarn et al., 2017, 2021; Liu & Wynne, 2019; Jiang et al., 2021, 2023; Zhao et al., 2022). Golovatch originally divided *Glyphiulus* into two species-groups, the *granulatus*-group and the *javanicus*-group, based on the structure of the first pair of legs in males (Golovatch et al., 2007a, b). The *granulatus*-group is distinguishable by its first pair of legs being devoid of median structures and instead featuring two widely separated prongs, along with often 1- or 2-segmented telopodite rudiments (Golovatch et al., 2007a). In contrast, the *javanicus*-group shared diagnostic characters of the first pair of legs in males provided with a medially contiguous, but not completely fused coxal processes, coupled with typically 4- or 5-segmented telopodites, as well as a unique carinotaxy patterns on the collum and subsequent metaterga (Golovatch et al., 2007b).

In a recent study by Zhao et al. (2022), the *javanicus*-group of Chinese *Glyphiulus* species was re-evaluated, resulting

Accepted by: Wendy Y. L. Wang

¹Program of Agriculture, Faculty of Agricultural Production, Maejo University, Chiang Mai 50290, Thailand

²Animal Systematics and Molecular Ecology Laboratory, Department of Biology, Faculty of Science, Mahidol University, Bangkok 10400, Thailand

³Animal Systematics Research Unit, Department of Biology, Faculty of Science, Chulalongkorn University, Bangkok 10330, Thailand

⁴Zoological Research Museum Alexander Koenig, Leibniz Institute for the Study of Biodiversity Change, Adenauerallee 160, 53113 Bonn, Germany; Email: t.wesener@leibniz-lib.de (*corresponding author)

in the separation of two new species groups: the *formosus*-group and the *sinensis*-group. This classification was based on the diagnostic characteristics of the male first pair of legs. The *formosus*-group is distinguished by the presence of a pair of small, fused, paramedian, subunciform projections that extend forward. These projections are accompanied by clearly separated, underdeveloped, 2-segmented leg vestiges. In contrast, the *sinensis*-group exhibits telopodites, which are often intact or nearly complete, with or without a claw. The coxosternum of the *sinensis*-group possesses a pair of relatively large and robust, paramedian outgrowths that are essentially unfused and extend laterally. Additionally, the *formosus*-group is uniquely defined by the presence of complete metatergal crests and a peculiar, I-III+P+M carinotaxy formula of the collum. It is noteworthy that the molecular phylogenetic relationship supports the morphological classification of these three species-groups, utilising their DNA sequences of four gene fragments: cytochrome oxidase subunit I (COI), 16S, 18S, and 28S.

The discovery of *Glyphiulus* species in Laos was first reported by Golovatch et al. (2007a) based on specimens collected between 1998 and 2000 by Anne Bedos and Louis Deharveng. *Glyphiulus bedosae* Golovatch, Geoffroy, Mauriès & VandenSpiegel, 2007, was described as the first Laotian cave-dwelling species found in Tham Pha Kouang Cave, Nong Kiaw (Muang Ngoy), Luang Prabang Province. This species belongs to the *granulatus*-group (Golovatch et al., 2007a).

Later, a further three species of the *javanicus*-group were described. These species are: 1) *G. costulifer* Golovatch, Geoffroy, Mauriès & VandenSpiegel, 2007, from the Tham Pha Kouang Cave, Nong Kiaw (Muang Ngoy), Luang Prabang Province; 2) *G. subcostulifer* Golovatch, Geoffroy, Mauriès & VandenSpiegel, 2007, from the Tham None Cave, Vang Vieng, Vientiane Province; and 3) *G. percostulifer* Golovatch, Geoffroy, Mauriès & VandenSpiegel, 2007, from the Tham Thê Cave, Ban Nakok (Nakhok), Khammouan Province (Golovatch et al., 2007b).

Likhitrakarn et al. (2017) have since described two more species of *Glyphiulus*: *G. subbedosae* Likhitrakarn, Golovatch & Panha, 2017 from the Kacham Waterfall, Chomphet District, Luang Prabang Province, belonging to the *granulatus*-group, and *G. semicostulifer* Likhitrakarn, Golovatch & Panha, 2017 from Kao Rao Cave, Viengphoukha District, Luang Namtha Province, belonging to the *javanicus*-group (Likhitrakarn et al., 2017). It is noteworthy that most of the *Glyphiulus* species in Laos appear to be troglomorphic cave dwellers, except for *G. subbedosae* which was discovered epigeically near waterfalls (Fig. 7).

In this study, detailed descriptions of three new *Glyphiulus* species from Laos are presented based on morphological and molecular analyses. The aim of these new integrative descriptions is to enhance our understanding of the biodiversity in this region by providing better insights into its overlooked species diversity. Additionally, a distributional

map and a key to all nine known species of the genus found in the country are also provided.

MATERIAL AND METHODS

Morphological studies

The specimens were collected in Laos during 2014 and 2016 as part of the biodiversity exploration for the Northern Lao-European Cave Project 2014 and the Hin Nam No Project. The collecting sites were located by GPS using the WGS84 datum. The taken specimens were euthanised using a two-step method following AVMA Guidelines for the Euthanasia of Animals (AVMA, 2020), before being preserved in 75%, later 95% ethanol for morphological and molecular studies. All specimens were examined, measured, and photographed under a Nikon SMZ 745T trinocular stereo microscope, equipped with a Canon EOS 5DS R digital SLR camera. The digital images obtained were processed and edited with Adobe Photoshop CS6. Line drawings were based on photographs which were taken with the stereo microscope equipped with a digital SLR camera.

The holotypes are housed in the Zoological Research Museum A. Koenig (ZFMK), Leibniz Institute for Animal Biodiversity, Bonn, Germany, while some of the paratypes are stored in the Museum of Zoology, Chulalongkorn University (CUMZ), Bangkok, Thailand, so that type specimens for future taxonomic research are available close to their area of occurrence in Asia.

The terminology used and the carinotaxic formulae in the descriptions follow those in Golovatch et al. (2007a, b; 2009; 2011a, b), while body ring counts are after Enghoff et al. (1993) and Golovatch et al. (2007a).

DNA extraction, PCR amplification and sequencing

DNA barcoding (Hebert et al., 2003) was conducted in order to establish species boundaries, and investigate intra- and interspecific barcode distances among the species described here. The DNA extraction, amplification, and sequencing of the cytochrome c oxidase subunit I gene (COI) was done following protocols employed in earlier studies (Sagorny & Wesener, 2017; Wesener, 2019), using the degenerate primer pair of the forward primer HCO-JJ (5'-AWA CTT CVG GRT GVC CAA ARA ATC A-3') and the reverse primer LCO-JJ (5'-CHA CWA AYC ATA AAG ATA TYG G-3') (Astrin & Stüben, 2008). Sequences were assembled, aligned and edited in BioEdit (Hall, 1999) or utilising the software Seqman (DNASTAR Inc.). BLAST searches (Altschul et al., 1997) were performed to confirm sequence identities and to check for any contamination. The whole dataset was translated into amino acids to rule-out the accidental amplification of pseudogenes. Eleven new sequences from six cambalid millipede species were successfully obtained and have been uploaded to GenBank under the accession codes OR359752–OR359762 (Table 1). PCR amplification was unsuccessful for one troglomorphic species, *Glyphiulus houaphanhensis*, new species, despite several attempts.

Table 1. The specimens included in the phylogenetic analysis. Abbreviations: CUMZ = Museum of Zoology, Chulalongkorn University; CAM = Cambalopsidae Project; JXK = Institute of Biology, Guizhou Academy of Sciences, Guiyang, China; MYR = Myriapoda; NP = National Park; SCAU = Zoological Collection of the South China Agricultural University; SMF = Senckenberg Museum für Naturkunde, Frankfurt, Germany; ZFMK = Zoological Research Museum Alexander Koenig, Bonn, Germany.

Species	Voucher number	GenBank #	Source
<i>Glyphiulus polytrichus</i> (Golovatch, Geoffroy, Mauriès & VandenSpiegel, 2011)	JXK222	MN725103.1	Jiang et al. 2021
<i>Hypocambala zizhong</i> Jiang, Guo, Chen & Xie, 2021	JXK165	MN725101.1	Jiang et al. 2021
<i>Pericambala sinica</i> (Zhang & Li, 1981)	JXK155	MN725100.1	Jiang et al. 2021
<i>Pericambala aramulus</i> (Zhang & Li, 1981)	JXK392	OP104953.1	Jiang et al. 2023
<i>Cambala annulata</i> (Say, 1821)	JXK517	MT683305.1	Jiang et al. 2021
<i>Plusioglyphiulus saksit</i> Golovatch, Geoffroy, Mauriès & VandenSpiegel, 2011	CUMZ CAM021	MN893781.1	Likhitrakarn et al. 2020
<i>Plusioglyphiulus erawan</i> Golovatch, Geoffroy, Mauriès & VandenSpiegel, 2011	CUMZ CAM031	MN893780.1	Likhitrakarn et al. 2020
<i>Trachyjulus singularis</i> (Attems, 1938)	CUMZ CAM107	MN893777.1	Likhitrakarn et al. 2020
<i>Trachyjulus magnus</i> Likhitrakarn, Golovatch, Jeratthitikul, Srisonchai, Sutcharit & Panha, 2020	CUMZ CAM070	MN893775.1	Likhitrakarn et al. 2020
<i>Trachyjulus unciger</i> Golovatch, Geoffroy, Mauriès & VandenSpiegel, 2012	CUMZ CAM079	MN893774.1	Likhitrakarn et al. 2020
<i>Trachyjulus phylloides</i> Golovatch, Geoffroy, Mauriès & VandenSpiegel, 2012	CUMZ CAM027	MN893773.1	Likhitrakarn et al. 2020
<i>Trachyjulus bifidus</i> Likhitrakarn, Golovatch, Srisonchai, Brehier, Lin, Sutcharit & Panha, 2018	CUMZ CAM061	MN893772.1	Likhitrakarn et al. 2020
<i>Glyphiulus duangdee</i> Golovatch, Geoffroy, Mauriès & VandenSpiegel, 2011	CUMZ CAM022	MN893779.1	Likhitrakarn et al. 2020
<i>Glyphiulus impletus</i> Jiang, Guo, Chen & Xie, 2018	SCAUWL39	ON255890.1	Zhao et al. 2022
<i>Glyphiulus calceus</i> Jiang, Guo, Chen & Xie, 2018	SCAUWL37	ON255888.1	Zhao et al. 2022
<i>Glyphiulus zorzini</i> Mauriès & Duy, 1997	SCAUWL23	ON255887.1	Zhao et al. 2022
<i>Glyphiulus speobius</i> Golovatch, Geoffroy, Mauriès & VandenSpiegel, 2011	SCAUWL62	ON255883.1	Zhao et al. 2022
<i>Glyphiulus proximus</i> Golovatch, Geoffroy, Mauriès & VandenSpiegel, 2011	SCAUWL61	ON255882.1	Zhao et al. 2022
<i>Glyphiulus deharvengi</i> Golovatch, Geoffroy, Mauriès & VandenSpiegel, 2007	SCAUWL15	ON255877.1	Zhao et al. 2022
<i>Glyphiulus granulatus</i> (Gervais, 1847)	JXK196	MN893780.1	Jiang et al. 2021
<i>Glyphiulus quadrohamatis</i> Cheng & Meng, 1991	JXK072	MN725099.1	Jiang et al. 2021
<i>Glyphiulus calceus</i> Jiang, Guo, Chen & Xie, 2018	JXK061	MN725098.1	Jiang et al. 2021
<i>Glyphiulus impletus</i> Jiang, Guo, Chen & Xie, 2018	JXK002	MN725095.1	Jiang et al. 2021
<i>Glyphiulus guangnanensis</i> Jiang, Guo, Chen & Xie, 2018	JXK051	MN725096.1	Jiang et al. 2021
<i>Glyphiulus foetidus</i> Jiang, Guo, Chen & Xie, 2018	JXK059	MN725097.1	Jiang et al. 2021
<i>Glyphiulus formosus</i> (Pocock, 1895)	JXK278	MN725178.1	Jiang et al. 2021
<i>Plusioglyphiulus steineri</i> Golovatch, Geoffroy, Mauriès & VandenSpiegel, 2009	SMF	OR359752	This study
<i>Plusioglyphiulus deharvengi</i> Golovatch, Geoffroy, Mauriès & VandenSpiegel, 2009	SMF	OR359753	This study

Species	Voucher number	GenBank #	Source
<i>Glyphiulus pseudocostulifer</i> , new species	ZFMK MYR9994A	OR359754	This study
<i>Glyphiulus pseudocostulifer</i> , new species	ZFMK MYR9994B	OR359755	This study
<i>Glyphiulus pseudocostulifer</i> , new species	ZFMK MYR10009A	OR359756	This study
<i>Glyphiulus pseudocostulifer</i> , new species	ZFMK MYR10004A	OR359757	This study
<i>Glyphiulus pseudocostulifer</i> , new species	ZFMK MYR10008	OR359758	This study
<i>Glyphiulus pseudocostulifer</i> , new species	CUMZ MYR10008A	OR359759	This study
<i>Glyphiulus steineri</i> , new species	ZFMK MYR6203	OR359760	This study
<i>Glyphiulus semicostulifer</i> Likhitrakarn, Golovatch & Panha, 2017	CUMZ CAM057	OR359761	This study
<i>Glyphiulus subbedosae</i> Likhitrakarn, Golovatch & Panha, 2017	CUMZ CAM058	OR359762	This study

Genetic analyses

Sequences were aligned and inspected using BioEdit (Hall, 1999). For the far outgroup, sequences from two species belonging to different families of the Cambalidea were retrieved from GenBank. In addition, we added all COI sequences of the family Cambalopsidae of sufficient quality and length available in GenBank (in June 2023), including 13 species of *Glyphiulus*, five species of *Trachyjulus* Peters, 1864, two species of *Phusioglyphiulus* Silvestri, 1923 and a single species of *Hypocambala* Silvestri, 1897 (see Table 1). The final aligned dataset comprised COI (671 bp) from 37 individual specimens.

In order to get insights on the species delineation pattern of the Cambalopsidae, a p-distance analysis was conducted on the 37 COI sequences. The number of base differences per site between sequences was calculated (see Table 2). Codon positions included were 1st+2nd+3rd. All ambiguous positions were removed for each sequence pair. The p-distance analysis was conducted in MEGA6 (Tamura et al., 2013).

In order to get an overview about the phylogenetic relationships of the newly described and sequenced species among the Cambalopsidae, a maximum likelihood analysis was conducted based on the same COI dataset. Phylogenetic analyses were also performed in MEGA6. The best fitting substitution model for a maximum likelihood analysis was calculated with Modeltest (Tamura & Nei, 1993) as implemented in MEGA6. The best fitting model was the general time reversible (GTR)-Model (Tavaré, 1986) with gamma distribution and invariant sites (GTR+G+I) (lnL = -8801.615, Invariant = 0.4301692, Gamma = 0.654062057, R = 4.456556; Freq A: 0.2929, T: 0.3355, C: 0.2166, G: 0.1547).

The rate variation model allowed for some sites to be evolutionarily invariable ([+I], 43.9404% sites). An initial tree for the heuristic search was obtained automatically by applying neighbour-joining and BioNJ algorithms to a matrix of pairwise distance estimated using the Maximum Likelihood Composite (MLC) approach. Codon positions included were 1st+2nd+3rd. All positions with less than 50%

site coverage were eliminated. The final dataset contained a total of 665 positions. The bootstrap consensus tree was inferred from 1000 replicates using standard bootstrap procedures (Felsenstein, 1985). The tree with the highest log likelihood (-8798.6551) is shown in Fig. 8. The obtained tree was edited in Adobe Illustrator CS2, with all bootstrap values >50% as well as any nodes relevant to taxa discussed in the text illustrated.

TAXONOMY

Family Cambalopsidae Cook, 1895

Genus *Glyphiulus* Gervais, 1847

Glyphiulus pseudocostulifer, new species (Figs. 1, 2)

Holotype. Male (ZFMK MYR-10009A (TW411)), Laos, Oudomxay Province, Ban Chom Ong, Tham Ketlin (F47-120-011), 20°43'19"N, 101°45'59"E, 28 December 2014, leg. M. Vandermeulen.

Paratypes. 1 female (ZFMK MYR-10009), same locality, together with holotype. 1 male (CUMZ MYR-10008A (TW414)), same locality, 27 December 2014, leg. M. Vandermeulen. 1 male (ZFMK MYR-9994A (TW400)) 1 female (ZFMK MYR-9994B (TW401)), Laos, Oudomxay Province, Ban Houay Soy, Tham Houay Soy (F47-120-015), 20°42'37"N, 101°45'50"E, 29 December 2014, leg. H. Steiner and I. Ermakova. 1 male (ZFMK MYR-10004A (TW412)), Laos, Oudomxay Province, Ban Chom Ong, Tham Hou Nguak (F47-120-010), 20°42'54"N, 101°45'38"E, 27 December 2014, leg. D. Fröhlich and M. Laumanns.

Etymology. To emphasise the obvious similarities to *G. costulifer* Golovatch, Geoffroy, Mauriès & VandenSpiegel, 2007. Noun in apposition.

Diagnosis. This new species is especially similar to both *G. steineri*, new species, and *G. costulifer*, from Luang Prabang Province, Laos (Golovatch et al., 2007b). With *G. costulifer*,

Table 2. Matrix of the average uncorrected p-distance (%) based on 671-bp COI barcoding region between 17 *Glyphiulus* species and some related taxa. Interspecific divergences (and intraspecific distances in the case of *G. pseudocostulifer*) are below the diagonal; intraspecific divergences are marked in bold.

Taxa	1	2	3	4	5	6	7	8	9	10	11	12	13	14	15	16	17	18	19	20	21	22	23	24	25	26	27	28	29	30	31	32	33	34	35	36		
<i>Glyphiulus polystichus</i> (JXK222)																																						
<i>Hypocambala zizhongii</i> (JXK165)	0.192																																					
<i>Percambala sinica</i> (JXK155)	0.230	0.214																																				
<i>Percambala aramulus</i> (JXK392)	0.228	0.214	0.002																																			
<i>Cambala annulata</i> (JXK517)	0.236	0.223	0.215	0.212																																		
<i>Plusioglyphiulus saksti</i> (CUMZ CAM021)	0.204	0.206	0.228	0.224	0.214																																	
<i>Plusioglyphiulus erawan</i> (CUMZ CAM031)	0.197	0.188	0.208	0.208	0.205	0.136																																
<i>Trachyiulus singularis</i> (CUMZ CAM107)	0.225	0.228	0.247	0.247	0.231	0.201	0.216																															
<i>Trachyiulus magnus</i> (CUMZ CAM070)	0.188	0.208	0.223	0.231	0.246	0.206	0.200	0.215																														
<i>Trachyiulus unceiger</i> (CUMZ CAM079)	0.232	0.245	0.230	0.239	0.223	0.243	0.246	0.238	0.206																													
<i>Trachyiulus phyllodes</i> (CUMZ CAM027)	0.214	0.203	0.217	0.220	0.215	0.216	0.206	0.207	0.200	0.195																												
<i>Trachyiulus bifidus</i> (CUMZ CAM061)	0.219	0.241	0.243	0.246	0.218	0.210	0.219	0.215	0.201	0.203	0.151																											
<i>Glyphiulus duangdee</i> (CUMZ CAM022)	0.195	0.195	0.223	0.227	0.222	0.212	0.195	0.235	0.237	0.227	0.213	0.212																										
<i>Glyphiulus impletus</i> (SCAUWL39)	0.221	0.251	0.245	0.239	0.234	0.203	0.220	0.197	0.227	0.247	0.233	0.224	0.233																									
<i>Glyphiulus calcens</i> (SCAUWL37)	0.224	0.230	0.254	0.248	0.221	0.208	0.213	0.216	0.219	0.262	0.210	0.215	0.231	0.142																								
<i>Glyphiulus zorini</i> (SCAUWL23)	0.166	0.190	0.243	0.242	0.206	0.178	0.174	0.239	0.221	0.248	0.207	0.199	0.181	0.210	0.211																							
<i>Glyphiulus speobius</i> (SCAUG62)	0.175	0.188	0.197	0.202	0.179	0.202	0.183	0.210	0.215	0.233	0.183	0.199	0.149	0.212	0.204	0.167																						
<i>Glyphiulus proximus</i> (SCAUG61)	0.171	0.195	0.212	0.215	0.202	0.183	0.175	0.227	0.189	0.228	0.181	0.198	0.181	0.212	0.196	0.170	0.122																					
<i>Glyphiulus deharvengi</i> (SCAUG15)	0.206	0.214	0.230	0.237	0.217	0.207	0.192	0.227	0.207	0.233	0.207	0.224	0.193	0.221	0.199	0.195	0.164	0.151																				
<i>Glyphiulus granulatus</i> (JXK196)	0.208	0.193	0.227	0.227	0.214	0.206	0.201	0.225	0.210	0.225	0.208	0.201	0.206	0.207	0.215	0.179	0.160	0.186	0.180																			
<i>Glyphiulus quadromatus</i> (JXK072)	0.201	0.204	0.234	0.234	0.206	0.192	0.184	0.227	0.208	0.245	0.179	0.201	0.169	0.229	0.215	0.177	0.171	0.182	0.158	0.199																		
<i>Glyphiulus calcens</i> (JXK061)	0.219	0.228	0.256	0.256	0.241	0.212	0.223	0.221	0.217	0.256	0.214	0.219	0.236	0.146	0.021	0.225	0.219	0.214	0.212	0.217	0.221																	

Taxa	1	2	3	4	5	6	7	8	9	10	11	12	13	14	15	16	17	18	19	20	21	22	23	24	25	26	27	28	29	30	31	32	33	34	35	36	
<i>Glyphilus impletus</i> (JXK002)	0.212	0.239	0.228	0.228	0.230	0.195	0.214	0.192	0.221	0.238	0.215	0.217	0.225	0.022	0.129	0.210	0.203	0.201	0.214	0.201	0.212	0.131															
<i>Glyphilus guangnanensis</i> (JXK051)	0.184	0.197	0.219	0.219	0.201	0.197	0.177	0.236	0.195	0.215	0.190	0.192	0.199	0.216	0.206	0.157	0.177	0.169	0.186	0.199	0.193	0.208	0.206														
<i>Glyphilus foetidus</i> (JXK059)	0.221	0.243	0.247	0.247	0.234	0.228	0.247	0.228	0.221	0.228	0.227	0.230	0.228	0.245	0.221	0.227	0.199	0.236	0.238	0.221	0.225	0.228	0.230	0.221													
<i>Glyphilus formosus</i> (JXK278)	0.215	0.219	0.247	0.239	0.231	0.211	0.233	0.224	0.208	0.271	0.217	0.219	0.220	0.166	0.168	0.205	0.210	0.205	0.227	0.215	0.210	0.168	0.157	0.221	0.225												
<i>Phacioglyphilus steineri</i> (SMF)	0.199	0.199	0.227	0.229	0.232	0.161	0.159	0.227	0.203	0.230	0.207	0.231	0.203	0.223	0.205	0.189	0.189	0.172	0.210	0.197	0.210	0.204	0.217	0.204	0.236	0.228											
<i>Phacioglyphilus deharvengi</i> (SMF)	0.199	0.203	0.208	0.207	0.214	0.122	0.128	0.204	0.210	0.228	0.206	0.194	0.194	0.205	0.209	0.177	0.183	0.175	0.195	0.188	0.186	0.212	0.197	0.196	0.216	0.208	0.167										
<i>Glyphilus pseudocostulifer</i> , new species (ZFMK MYR8994A)	0.184	0.223	0.230	0.236	0.222	0.210	0.206	0.235	0.227	0.247	0.204	0.222	0.225	0.233	0.231	0.198	0.175	0.193	0.225	0.212	0.217	0.238	0.212	0.175	0.221	0.261	0.216	0.212									
<i>Glyphilus pseudocostulifer</i> , new species (ZFMK MYR8994B)	0.186	0.223	0.238	0.243	0.223	0.218	0.209	0.240	0.230	0.251	0.209	0.224	0.228	0.240	0.233	0.203	0.184	0.200	0.230	0.218	0.218	0.244	0.218	0.179	0.231	0.260	0.222	0.217	0.012								
<i>Glyphilus pseudocostulifer</i> , new species (ZFMK MYR10009A)	0.169	0.217	0.227	0.231	0.215	0.212	0.199	0.240	0.221	0.234	0.201	0.212	0.228	0.241	0.233	0.193	0.186	0.192	0.219	0.201	0.221	0.234	0.214	0.166	0.208	0.250	0.222	0.215	0.057	0.064							
<i>Glyphilus pseudocostulifer</i> , new species (ZFMK MYR0004A)	0.188	0.227	0.243	0.246	0.228	0.215	0.210	0.246	0.235	0.252	0.212	0.231	0.232	0.242	0.239	0.202	0.183	0.199	0.237	0.221	0.225	0.247	0.221	0.184	0.230	0.271	0.222	0.221	0.024	0.036	0.069						
<i>Glyphilus pseudocostulifer</i> , new species (ZFMK MYR10008)	0.169	0.214	0.228	0.234	0.215	0.210	0.198	0.238	0.221	0.234	0.207	0.209	0.224	0.238	0.241	0.195	0.186	0.193	0.224	0.199	0.221	0.239	0.212	0.171	0.214	0.255	0.221	0.215	0.057	0.064	0.009	0.066					
<i>Glyphilus pseudocostulifer</i> , new species (ZFMK MYR10008A)	0.169	0.217	0.227	0.231	0.215	0.209	0.197	0.240	0.221	0.238	0.206	0.215	0.228	0.241	0.238	0.192	0.184	0.192	0.225	0.204	0.223	0.239	0.215	0.171	0.212	0.254	0.219	0.213	0.055	0.066	0.010	0.058	0.010				
<i>Glyphilus steineri</i> , new species (ZFMK MYR6203)	0.184	0.204	0.227	0.229	0.234	0.201	0.212	0.219	0.237	0.261	0.215	0.231	0.197	0.232	0.221	0.201	0.198	0.196	0.218	0.210	0.206	0.221	0.227	0.166	0.212	0.222	0.209	0.207	0.206	0.209	0.204	0.216	0.204	0.203			
<i>Glyphilus semicostulifer</i> (CUMZ CAM057)	0.186	0.188	0.208	0.215	0.217	0.191	0.173	0.242	0.204	0.237	0.210	0.219	0.209	0.235	0.229	0.168	0.204	0.172	0.209	0.184	0.192	0.225	0.225	0.149	0.234	0.224	0.200	0.185	0.181	0.185	0.188	0.187	0.188	0.188	0.176		
<i>Glyphilus subdorsae</i> (CUMZ CAM058)	0.197	0.203	0.247	0.244	0.225	0.210	0.200	0.242	0.222	0.257	0.225	0.228	0.166	0.242	0.217	0.189	0.190	0.195	0.209	0.204	0.201	0.221	0.232	0.188	0.197	0.230	0.219	0.208	0.216	0.216	0.214	0.223	0.219	0.219	0.193	0.188	

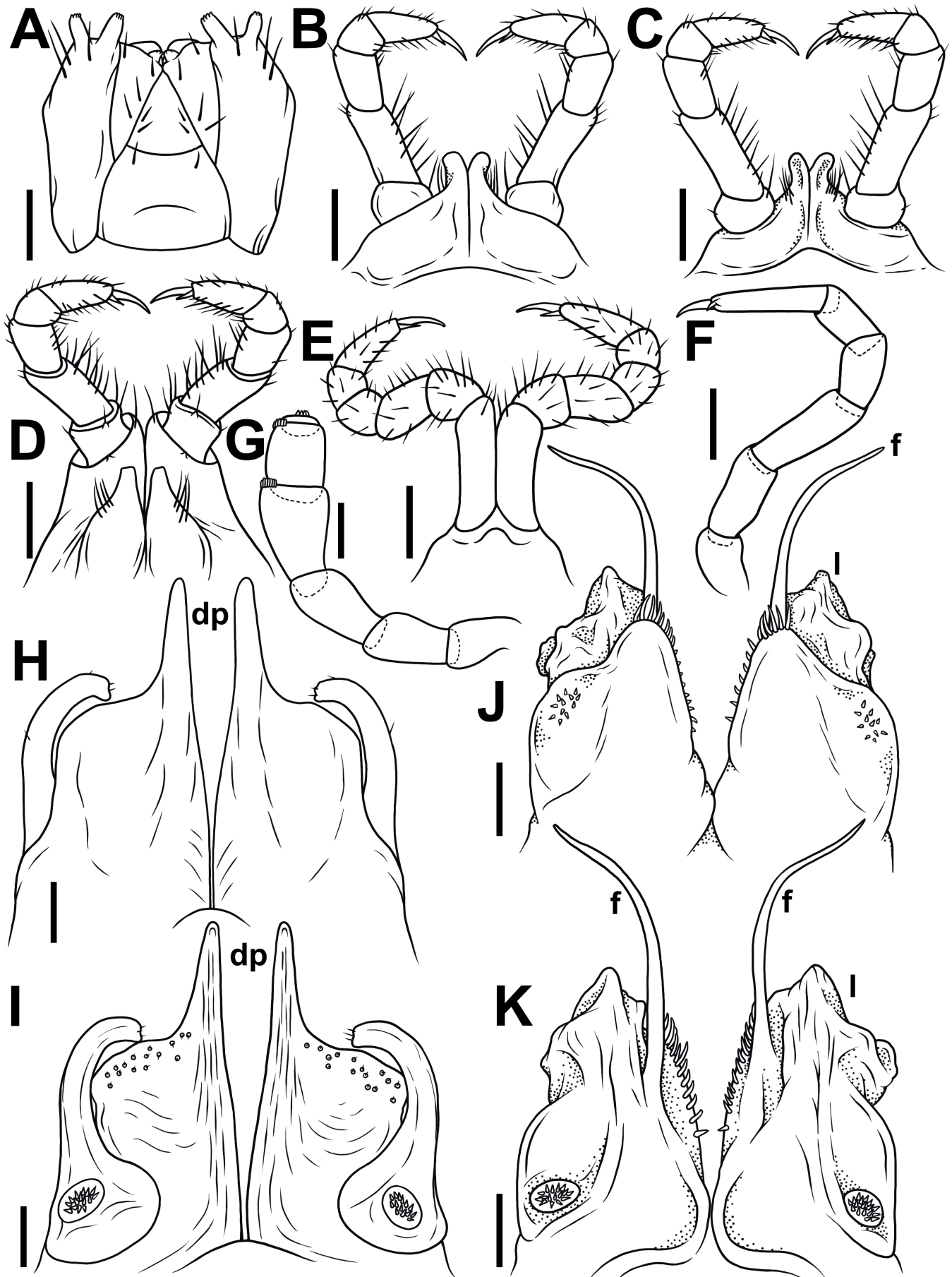


Fig. 2. *Glyphiulus pseudocostulifer*, new species, male holotype (ZFMK MYR10009A). A, gnathochilarium, ventral view; B, C, leg pair 1, oral and caudal views, respectively; D, leg pair 2, caudal view; E, leg pair 3, caudal view; F, midbody leg; G, antenna, lateral view; H, I, anterior gonopods, oral and caudal views, respectively; J, K, posterior gonopods, oral and caudal views, respectively. Abbreviations: ap, apicolateral process; dp, apicomasal processes; f, flagellum process; l, lamelliform lobe. Scale bar: A–G 0.1 mm, H–K 0.02 mm.

and digitiform) and the presence of a very long and slender flagellum process (f) on the posterior gonopods (Fig. 2J, K) (vs. a shorter flagellum process). The differences between *G. pseudocostulifer*, new species, and *G. steineri*, new species, are found in the carinotaxic formula of the midbody rings as well as the gonopods (see further details below).

Description. Length of holotype 26.5 mm; adult paratypes 17.5–29.5 (males) or 20.8–27.5 mm long (females); midbody rings/segments round in cross-section (Fig. 1F), their width (horizontal diameter) and height (vertical diameter) being similar; width in holotype 0.9 mm; in paratypes 1.0–1.3 (males) or 1.1–1.5 (females).

Colouration in alcohol (Fig. 1), after nine years of preservation, uniformly greenish-golden to grey-brown, dorsal crests and porosteles usually dark brownish (Fig. 1A, B, D, E, G, H). Head light yellow, vertex dark brown to red brownish (Fig. 1A, C). Antennae, venter and legs yellowish to yellow brown (Fig. 1A–C, E–G, I). Eyes blackish (Fig. 1A, C).

Body with 60p+2a+T (holotype) rings; paratypes with 34–52p+5a+T (males) or 44–57p+2–6a+T (females). Eye patches transversely ovoid, each composed of 7–11 blackish, rather flat ommatidia in 3–5 irregular longitudinal rows (Fig. 1A). Antennae rather short and clavate (Figs. 1A, C, 2G), extending to ring 4 laterally, antennomeres 5 and 6 each with a small distoventral group or corolla of bacilliform sensilla (Fig. 2H). Gnathochilarium with a clearly separated promontum (Fig. 2A).

Head width = ring 2 < collum = midbody ring (close to 13th to 15th) >> ring 4 < 5 < 6 < 7 < 8 < 9 < 10; body abruptly tapering towards telson on a few posterior-most rings (Fig. 1H). Postcollar constriction evident (Fig. 1B).

Collum with low evident crests, carinotaxy formula 1–5+6a+pc+ma (Fig. 1A–C), with 6+6 longitudinal crests starting from anterior edge, but both median crests interrupted at about caudal 1/4–1/3, being replaced there by 1+1+1 crests starting from posterior edge, lateral crests being longer than median one.

Following metaterga similarly strongly crested (Fig. 1A–H), especially from ring 5 on, whence porosteles commence (Fig. 1A, B), smaller tubercles in their stead on legless rings in front of telson due to lack of ozopores (Fig. 1G, H). Porosteles large, conical, round, directed caudolaterad, wider than high, ozoporiferous crests distinctly divided into two about midway, their frontal halves being higher (Fig. 1A, B, D–H). Carinotaxy formulae 2+I/i+3/3+I/i+2 on rings 2 and 3, as well as on the last 1 or 2 leg-bearing and legless rings (Fig. 1A, B, G, H); midbody rings showing all dorsal crests subdivided transversely (carinotaxy formulae 2/2+I/i+3/3+I/i+2/2) and sharper, especially so lateral crests (Fig. 1D, E, G, H).

Tegument finely alveolate-areolate (Fig. 1A, B, D, E, G, H), dull throughout. Fine longitudinal striations in front of stricture between pro- and metazonae, remaining surface of prozonae very delicately shagreened (Fig. 1D, E). Metatergal setae absent. Rings 2 and 3 with long pleural flaps.

Epiproct (Fig. 1G–I) simple, regularly rounded caudally, faintly convex medially, with a rounded ridge in caudal part and an evident axial rib dorsally. Paraprocts regularly

convex, each with premarginal sulci medially and a row of sparse setae at medial margin (Fig. 1I). Hypoproct slightly concave caudally, with 1+1 strongly separated setae near caudal margin (Fig. 1I).

Ventral flaps behind gonopod aperture on male ring 7 evident, distinguishable as rather low swellings with rounded flaps bent abruptly caudad (Fig. 1C).

Legs rather short and stout, on midbody rings about 3/4–3/5 as long as body diameter (Figs. 1A, C, G, I, 2F). Claw at base with an evident accessory claw about 1/3–1/4 the length of main claw.

Male leg pair 1 highly characteristic (Fig. 2B, C) in showing nearly fully developed, 5-segmented telopodites and a pair of rather small, subdigitiform, medially contiguous, but apically diverging coxal processes, higher than prefemur (Fig. 2B, C), with a group of a few strong setae at base.

Male leg pair 2 nearly normal, claw long and slender, coxa somewhat reduced, femur abbreviated on frontal face; penes broad, oblong-subtrapeziform, each with 4 or 5 setae distolaterally (Fig. 2D).

Male leg pair 3 modified, coxa especially slender and elongate (Fig. 2E).

Anterior gonopods (Fig. 2H, I) with a typical shield-like coxosternum, this being rather densely microsetose on caudal face (Fig. 2I), with a long and high, digitiform, apicomeral process (dp). Telopodite typical, rather small, slender, movable, 1-segmented, lateral in position, with 3 or 4 strong apical setae and a field of microsetae at base (Fig. 2I).

Posterior gonopods (Fig. 2J, K) compact, subtrapezoid, micropapillate medially on oral face (Fig. 2K); with a very long and slim flagellum process (f), a pointed tip (Fig. 2J, K); a lamelliform lobe (l) higher than caudal piece of coxite (Fig. 2J), membranous, wrinkled frontolaterally, with an apical field of coniform microsetae caudally (Fig. 2K). Coxite rather smooth, each mediolateral part of coxite with 13–17 strong, short and curved setae (Fig. 2J, K).

Glyphiulus steineri, new species

(Figs. 3, 4)

Holotype. Male (ZFMK MYR-6203 (TW408)), Laos, Khammouan Province, Tham Nam Ock, 17°35'24.11"N, 105°50'7.26"E, 3 March 2016, leg. H. Steiner.

Etymology. To honour the German collector and biospeleologist Helmut Steiner, an active explorer of the caves of Laos, noun.

Diagnosis. This new species is especially similar to *G. pseudocostulifer*, new species, with which it shares the following diagnostic characters: the unique carinotaxic formulae of postcollum rings, coupled with anterior and posterior gonopod structural details. It differs from *G. pseudocostulifer*, new species, by the carinotaxic formula of the midbody rings: 2/2+I/i+3/3+I/i+2/2 (Fig. 3A, B, D–H) (vs. 2+I/i+3/3+I/i+2 (Fig. 1A, B, D–H)), coupled with the apicomeral processes (d) on the anterior gonopods being broader and stout (Fig. 4H, I) (vs. longer and slender (Fig. 2H, I)), and with an evident, swollen, rounded apicolateral process (ap) (Fig. 4H, I) (vs. smooth without apicolateral

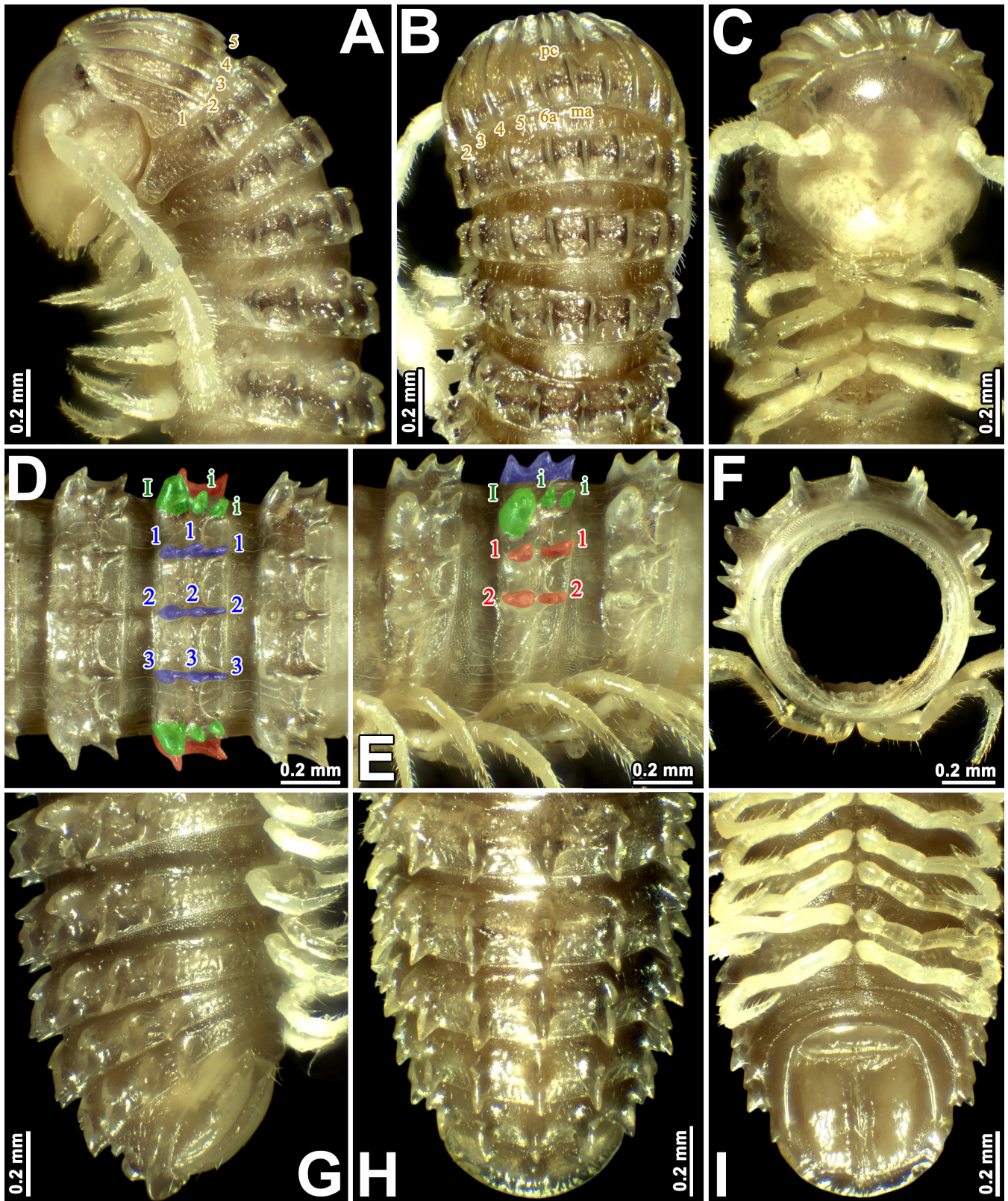


Fig. 3. *Glyphiulus steineri*, new species, male holotype (ZFMK MYR6203). A–C, anterior part of body, lateral, dorsal, and ventral views, respectively; D, E, midbody rings, dorsal and lateral views, respectively; F, cross-section of a midbody ring; G–I, posterior part of body, lateral, dorsal, and ventral views, respectively.

process (Fig. 2H, I)), and the axe-shaped tip of the flagellum process (f) on the posterior gonopods (Fig. 4J, K) (vs. pointed tip (Fig. 2J, K)).

Description. Length of holotype 34.5 mm; midbody rings round in cross-section (Fig. 3F), their width (horizontal diameter) and height (vertical diameter) being similar; width of holotype 1.4 mm.

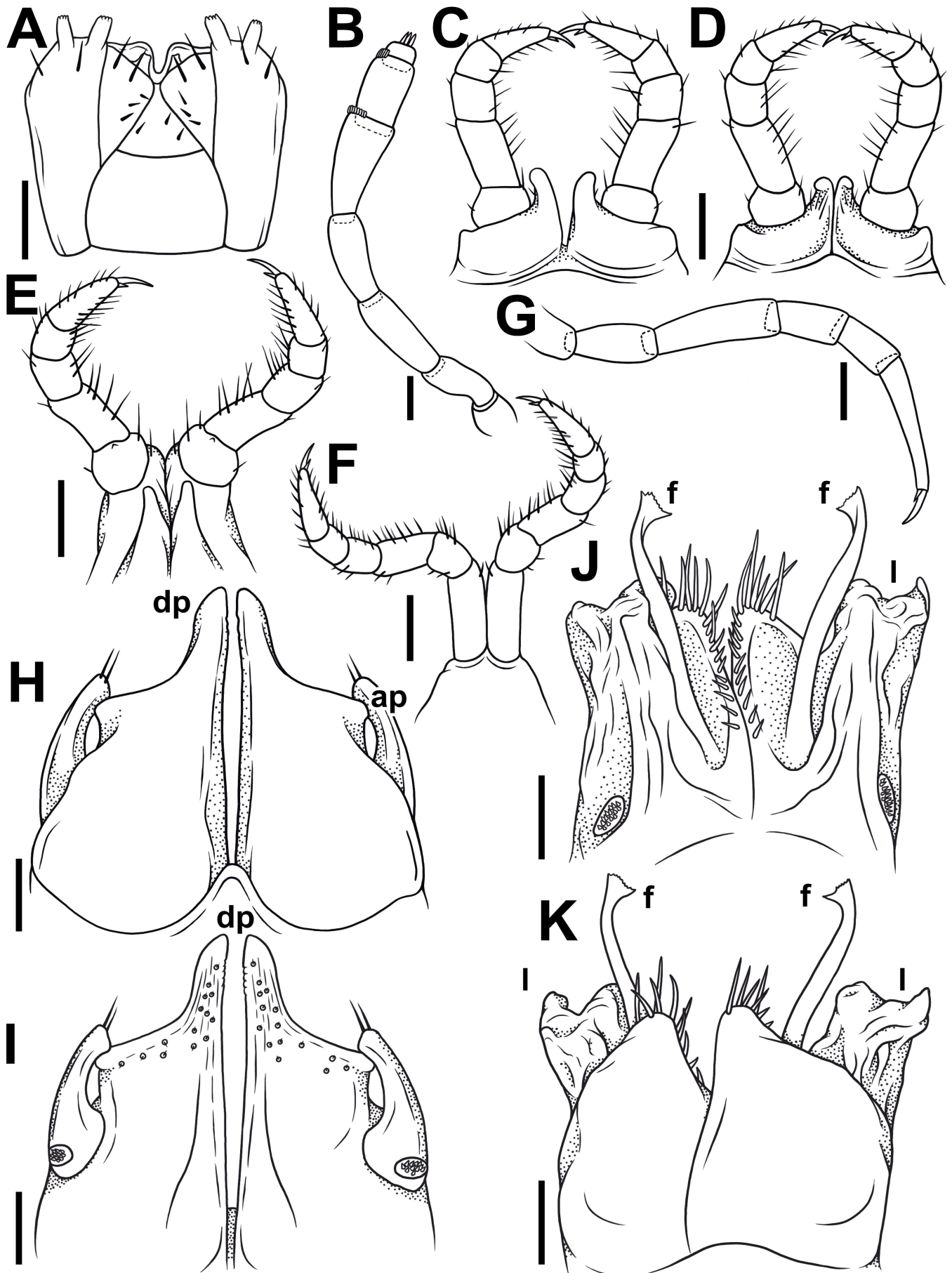


Fig. 4. *Glyphiulus steineri*, new species, male holotype (ZFMK MYR6203). A, gnathochilarium, ventral view; Bm antenna, lateral view; C, D, leg pair 1, oral and caudal views, respectively; E, leg pair 2, caudal view; F, leg pair 3, caudal view; G, midbody leg; H, I, anterior gonopods, oral and caudal views, respectively; J, K, posterior gonopods, caudal and oral views, respectively. Abbreviations: ap, apicolateral process; dp, apicomesal processes; f, flagellum process; l, lamelliiform lobe. Scale bar: A–G 0.1 mm, H–K 0.02 mm.

Colouration in alcohol (Fig. 3), after seven years of preservation, uniformly brownish to yellowish, metazonites usually dark brownish (Fig. 3A, B, D, E, H). Head light brown yellowish, vertex dark brown (Fig. 3A, C). Antennae, venter, and legs yellowish to pallid (Fig. 3A–C, E–G, I). Eyes blackish (Fig. 3A, C).

Body with 56p+2a+T rings (holotype). Eye patches transversely ovoid, each composed of 3 or 4 rather flat ommatidia in a single longitudinal row (Fig. 3A, C). Antennae long and filiform (Figs. 3A–C, 4B), reaching beyond ring 6 laterally, antennomeres 5 and 6 each with a small distoventral group or corolla of bacilliform sensilla (Fig. 4B). Gnathochilarium with a clearly separated promentum (Fig. 4A).

Head width = ring 2 < collum = midbody ring (close to 8th to 10th) > ring 3 = 6 > 4 = 5 < 7 < 8 = 10; body abruptly tapering towards telson on a few posterior-most rings (Fig. 3H). Postcollar constriction rather evident (Fig. 3B).

Collum with 6+6 low longitudinal crests starting from anterior edge, but both median crests interrupted in about caudal 1/2–1/3, being replaced there by similar 1+1+1 crests; carinotaxy formula 1–5+6a+pc+ma (Fig. 3A–C).

Following metaterga very strongly crested (Fig. 3A–H), especially from ring 5 on, whence porosteles commence (Fig. 3A, B), each tubercle higher and more pointed tip (Fig. 3D, E), but smaller tubercles in their stead on legless rings in front of telson due to loss of ozopores (Fig. 3G, H). Porosteles large, conical, triangle, directed caudolaterad, higher than wide, ozoporiferous crests distinctly divided into three, their frontal porosteles half of metatergal height (Fig. 3D–H). Carinotaxy formulae 2+I/i+3+I/i+2 on rings 2 and 3, as well as on the last 1 or 2 leg-bearing and legless rings (Fig. 3A, B, G, H); midbody rings showing all dorsal crests subdivided transversely (carinotaxy formulae 2/2+I/i/i+3/3+I/i/i+2/2) and sharper, lateral crests especially sharp (Fig. 3D–H).

Tegument rather smooth and shining throughout, quite sparsely alveolate-areolate (Fig. 3A, B, D, E, G, H). Fine longitudinal striations in front of stricture between pro- and metazonae, remaining surface of prozonae very delicately shagreened (Fig. 3D, E). Metatergal setae absent. Rings 2 and 3 each with long pleural flaps. Epiproct (Fig. 3G–I) simple, regularly rounded caudally, faintly convex medially, with a median tubercle and a following rounded ridge in caudal part and an evident axial rib dorsally. Paraprocts regularly convex, each with premarginal sulci medially and a row of sparse setae at medial margin (Fig. 3I). Hypoproct smooth and straight caudally, with 1+1 strongly separated setae near caudal margin (Fig. 3I).

Ventral flaps behind gonopod aperture on male ring 7 evident, distinguishable as rather high swellings with rounded flaps bent abruptly caudad (Fig. 3C).

Legs long and slender, on midbody rings nearly as long as body diameter (Figs. 3A, C, F, G, H, 4G). Claw at base with an evident accessory claw about 1/3–1/4 the length of main claw (Fig. 4G).

Male leg pair 1 highly characteristic (Fig. 4C, D) in showing nearly fully developed, 5-segmented telopodites and a pair of rather small, subdigitiform, medially contiguous, but

apically diverging coxal processes with a group of few strong setae at base.

Male leg pair 2 nearly normal, claw long and slender, anteriorly, coxa somewhat reduced, and femur abbreviated on frontal face; penes broad, subtrapeziform, truncate apically, fused at base (Fig. 4E).

Male leg pair 3 modified, coxa especially slender and elongate (Fig. 4F).

Anterior gonopods (Fig. 4H, I) with a typical shield-like coxosternum, the latter moderately microsetose in anterior and medial parts on caudal face (Fig. 4I), with a long, high, digitiform, apicomesal process (dp) and an obvious apicolateral process (ap). Telopodite typical, rather small, slender, movable, 1-segmented, lateral in position, with 2 or 3 strong apical setae and a field of microsetae at base (Fig. 4I). Posterior gonopods (Fig. 4J, K) compact, broadly subquadrate, with a long, stout flagellum process (f), axe-shape tip (Fig. 4J, K); lamelliform lobe (l) higher than caudal piece of coxite, membranous, wrinkled frontolaterally, with an apical field of coniform microsetae caudally (Fig. 4J). Coxite smooth, each mediolateral part of coxite with 14–16 strong, long and curved setae (Fig. 4J, K).

Glyphiulus houaphanhensis, new species

(Figs. 5, 6)

Holotype. Male (ZFMK MYR-10011C), Laos, Houaphan Province, Xam Neua, Tham Lo (F48-125-119), 20°33'31.1"N, 104°01'24.2"E, 9 January 2014, leg. H. Steiner.

Paratypes. 1 male (CUMZ MYR-10005A), 1 male (ZFMK MYR-10001A), Laos, Houaphan Province, Xam Neua, Tham Long Ngeuang (F48-125-132), 20°32'20.1"N, 104°01'45.2"E, 15 January 2014, leg. H. Steiner. 1 female (ZFMK MYR-10000A), Laos, Houaphan Province, Xam Neua, Tham Falang (F48-125-122), 20°33'29.9"N, 104°01'25.5"E, 9 January 2014, leg. H. Steiner. 1 male, 2 females (ZFMK MYR-9999), Laos, Houaphan Province, Xam Neua, Tham Bae (F48-125-117), 20°33'50.8"N, 104°03'30.7"E, 7 January 2014, leg. H. Steiner.

Etymology. The species is named in allusion to the type locality — Houaphan Province, adjective.

Diagnosis. This new species is especially similar to *G. percostulifer* Golovatch, Geoffroy, Mauriès & VandenSpiegel, 2007, from Khammouan Province, Laos (Golovatch et al., 2007b), with which it shares the following diagnostic characters: the unique carinotaxic formula of midbody rings, coupled with anterior and posterior gonopod structural details. It differs from *G. percostulifer* by the absence of ommatidia (vs. present in *G. percostulifer*), the carinotaxic formula of the collum: 1+2c+3–4+5c+6a+pc+ma (Fig. 5A, B) (vs. 1–4+5a+pc+ma), coupled with the apicomesal processes (d) on the anterior gonopods being long and slender (Fig. 6H, I) (vs. broad and stout), and the apicolateral process (ap) on the anterior gonopods being large, curved and subdigitiform (Fig. 6H, I) (vs. small and rounded), and the presence of a slim and smooth flagellum process (f), with a pointed tip on

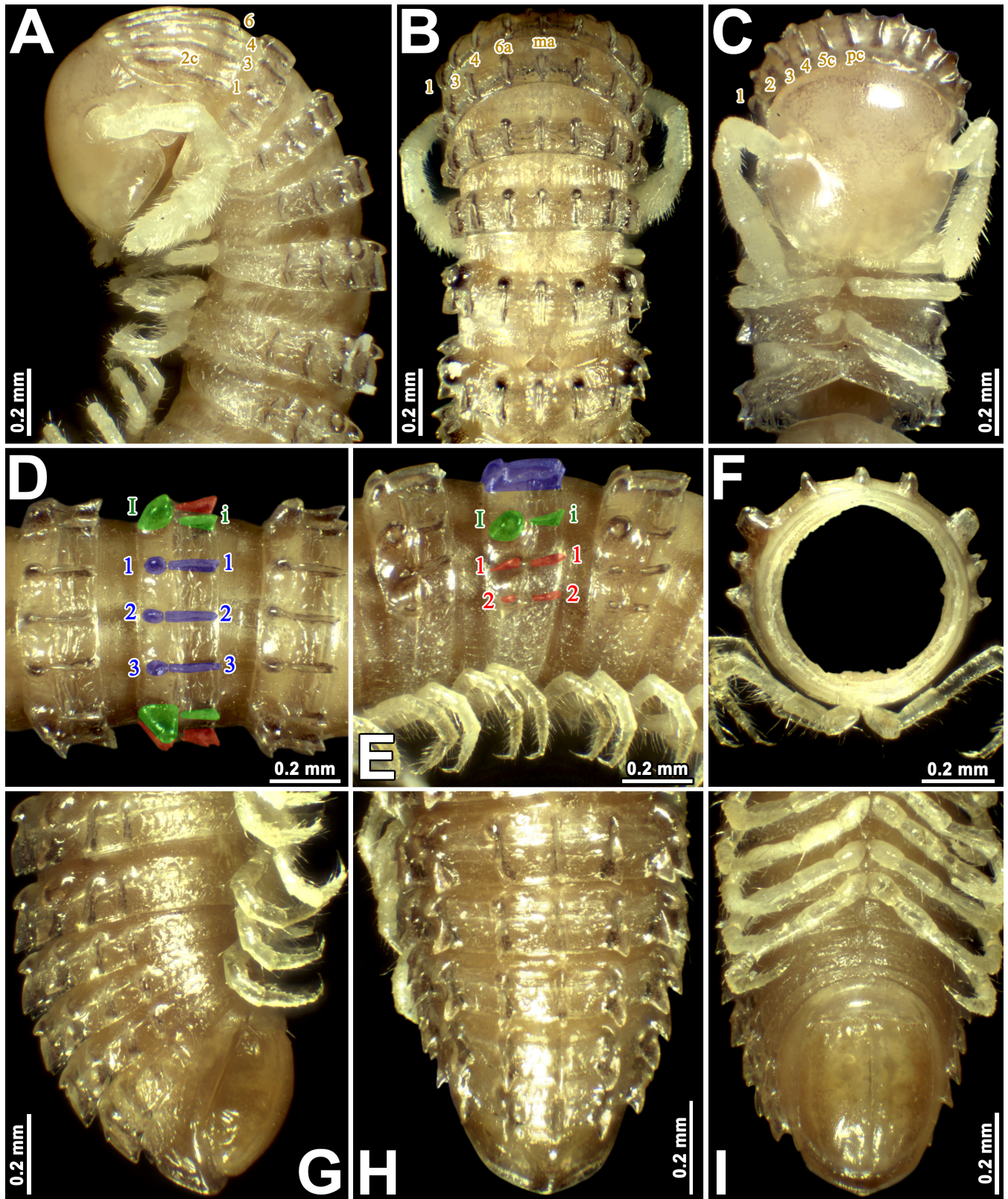


Fig. 5. *Glyphiulus houaphanhensis*, new species, male holotype (ZFMK MYR10011C). A–C, anterior part of body, lateral, dorsal, and ventral views, respectively; D, E, midbody rings, dorsal and lateral views, respectively; F, cross-section of a midbody ring; G–I, posterior part of body, lateral, dorsal, and ventral views, respectively.

the posterior gonopods (Fig. 6J, K) (vs. flagellum process plumose distally).

Description. Length of holotype 21.8 mm; that of paratypes 18.5–22.5 (males) or 18.5–22.8 mm (females); midbody

rings round in cross-section (Fig. 5F), their width (horizontal diameter) and height (vertical diameter) being similar; width of holotype 0.7 mm, of paratypes 0.9–1.0 (males) or 1.1–1.3 mm (females).

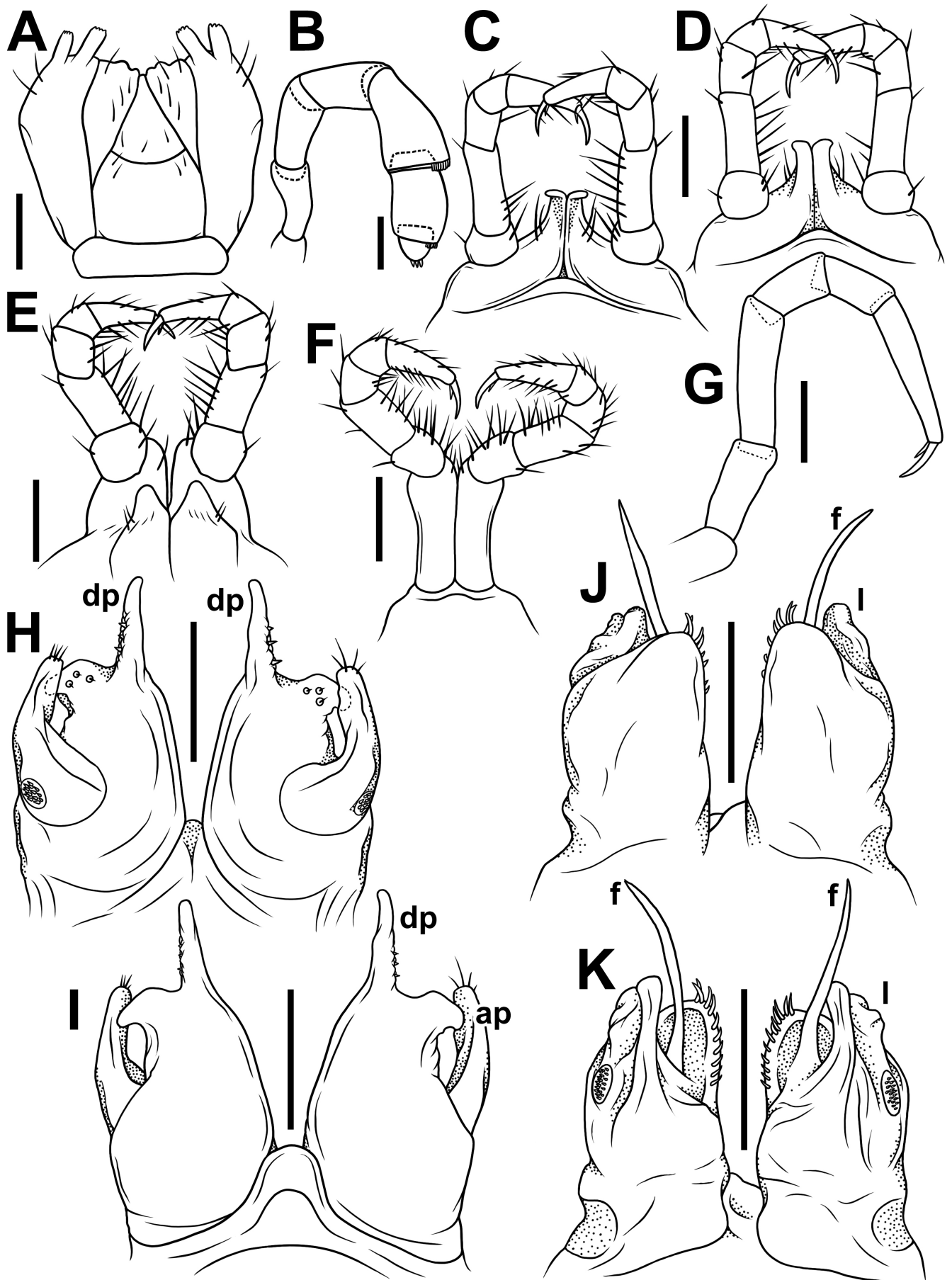


Fig. 6. *Glyphiulus houaphanhensis*, new species, male holotype (ZFMK MYR10011C). A, gnathochilarium, ventral view; B, antenna, lateral view; C, D, leg pair 1, caudal and oral views, respectively; E, leg pair 2, caudal view; F, leg pair 3, caudal view; G, midbody leg; H, I, anterior gonopods, caudal and oral views, respectively; J, K, posterior gonopods, oral and caudal views, respectively. Abbreviations: ap, apicolateral process; dp, apicomeres; f, flagellum process; l, lamelliform lobe. Scale bar: 0.1 mm.

Colouration in alcohol (Fig. 5), after nine years of preservation, uniformly brownish or chestnut-brown to pallid, dorsal crests and porosteles usually dark brownish (Fig. 5A–E, G, H). Head, antennae, venter, and legs yellowish to pallid (Fig. 5A–C, E–G, I).

Body with 46p+4a+T rings (holotype); paratypes with 37–44p+4a+T (males) or 40–50p+3–4a+T (females) rings. Eye patches invisible (Fig. 5A, C). Antennae long and clavate (Figs. 5A–C, 6B), reaching behind ring 5 laterally, antennomeres 5 and 6 each with a small distoventral group or corolla of bacilliform sensilla (Fig. 6B). Gnathochilarium with a clearly separated promentum (Fig. 6A).

Head width = ring 3 = 6 > 4 = 5 < 7 = collum < midbody ring (close to 8th to 10th); body abruptly tapering towards telson on a few posteriormost rings (Fig. 5H). Postcollar constriction rather evident (Fig. 5B).

Collum with evident crested, carinotaxy formula 1+2c+3–4+5c+6a+pc+ma (Fig. 5A–C), with 6+6 longitudinal crests starting from anterior edge, but both median crests interrupted in about caudal 2/3–3/4, being replaced there by similar 1+1+1 crests.

Following metaterga similarly strongly crested (Fig. 5A–H), especially from ring 5 on, whence porosteles commence (Fig. 5A, B), smaller tubercles in their stead on legless rings in front of telson due to lack of ozopores (Fig. 5G, H). Porosteles large, conical, round, directed caudolaterad, wider than high, ozoporiferous crests distinctly divided into two about midway, their frontal halves being higher (Fig. 5A, B, D–H). Carinotaxy formulae 2+I/i+3+I/i+2 on rings 2–4, as well as on the last 1 or 2 leg-bearing and legless rings (Fig. 5A, B, G, H); midbody rings showing all dorsal crests subdivided transversely (carinotaxy formulae 2/2+I/i+3/3+I/i+2/2) and sharper, especially so lateral crests (Fig. 5D–H). Tegument rather smooth and shining, quite sparsely alveolate-areolate (Fig. 5A, B, D, E, G, H). Fine longitudinal striations in front of stricture between pro- and metazonae, remaining surface of prozonae very delicately shagreened (Fig. 5D, E). Metatergal setae absent. Rings 2 and 3 each with long pleural flaps. Epiproct (Fig. 5G–I) simple, regularly rounded caudally, faintly convex medially, with a rounded ridge in caudal part and an evident axial rib dorsally. Paraprocts regularly convex, each with premarginal sulci medially and a row of sparse setae at medial margin (Fig. 5I). Hypoproct transversely bean-shaped, slightly concave caudally, with 1+1 strongly separated setae near caudal margin (Fig. 5I). Ventral flaps behind gonopod aperture on male ring 7 evident, distinguishable as low swellings forming no marked transverse ridge (Fig. 5C).

Legs long and slender, on midbody rings nearly as long as body diameter (Figs. 5A, C, E–G, I, 6G). Claw at base with a strong accessory spine almost half as long as main claw (Fig. 6G).

Male leg pair 1 highly characteristic (Fig. 6C, D) in showing nearly fully developed, 5-segmented telopodites and a pair of rather high, subdigitiform, medially contiguous, but apically diverging coxal processes with a group of few strong setae at base.

Male leg pair 2 nearly normal, claw long and slender, anteriorly, coxa somewhat reduced, and femur abbreviated on frontal face; penes broad, oblong-subtrapeziform, each with 2 or 3 strong setae distolaterally (Fig. 6E).

Male leg pair 3 modified, coxa especially slender and elongate (Fig. 6F).

Anterior gonopods (Fig. 6H, I) with a typical shield-like coxosternum, the latter sparsely microsetose in anterior and lateral parts on caudal face (Fig. 6I), with a long, high, digitiform, apicomeral process (dp) and an obvious, curved, apicolateral process (ap). Telopodite typical, rather small, slender, movable, 1-segmented, lateral in position, with 2 or 3 strong apical setae and a field of microsetae at base (Fig. 6I). Posterior gonopods (Fig. 6J, K) compact, subtrapezoid, with a rather long, slim flagellum process (f), pointed tip (Fig. 6J, K; lamelliform lobe (l) higher than caudal piece of coxite, membranous, wrinkled frontolaterally, with an apical field of coniform microsetae laterally (Fig. 6K). Coxite smooth, each mediolateral part of coxite with 10–12 strong, short, and curved setae (Fig. 6J, K).

Remarks. Based on its uniform colouration lacking any discernible patterns and the absence of eyes, this species appears to have undergone evolutionary adaptations indicative of troglomorphy. It is exclusively reported within the confined cave systems in the Xam Neua area of Houaphan Province (Fig. 7), Laos, unequivocally establishing its status as a species endemic to Laos.

Glyphiulus sp. 1

Material examined. 1 female (ZFMK MYR-10011A), 1 female (ZFMK MYR-10011B), Laos, Houaphan Province, Xam Neua, Tham Lo (F48-125-119), 20°33'31.1"N, 104°01'24.2"E, 9 January 2014, leg. H. Steiner.

Remarks. Based on somatic characteristics alone, these specimens resemble the members of the genus *Glyphiulus* described from Laos. This species lives in direct sympatry to *Glyphiulus houaphanhensis*, new species (Fig. 7), a rare occurrence in Cambalopsidae species. We do not name this species because only a female is available.

Glyphiulus sp. 2

Material examined. 1 female, 1 juvenile (Dwarf-SMF), Laos, Luang Prabang Province, Southeast Luang Prabang, Nam Khan, Xieng Ngeun District, Ban Keng Koun, 372 m a.s.l., 19°40'9.63"N, 102°18'4.42"E, 21–23 February 2008, leg. P. Jäger.

Remarks. According to the somatic characteristics, these specimens resemble members of the genus *Glyphiulus* described from Laos. However, despite the characteristic morphology combining a very small body size with the peculiar presence of just two ommatidia, we refrain from assigning a specific designation to this species due to the limited availability of only a female and an immature male.

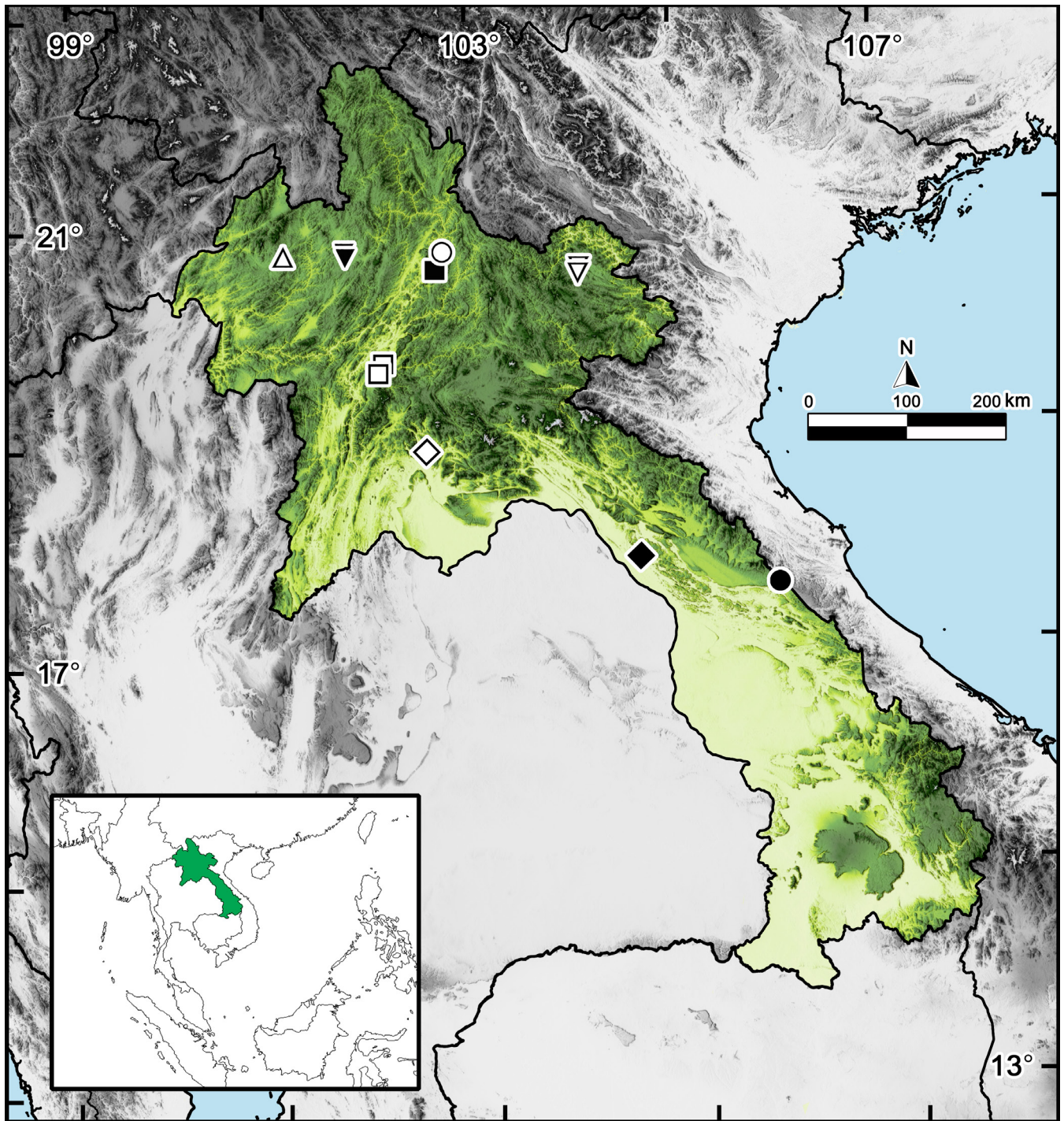


Fig. 7. Distribution of *Glyphiulus* species in Laos (9 species). \triangle : *Glyphiulus semicostulifer* Likhitrakarn, Golovatch & Panha, 2017; ∇ : *Glyphiulus pseudocostulifer*, new species; \circ : *Glyphiulus costulifer* Golovatch, Geoffroy, Mauriès & VandenSpiegel, 2007; \blacksquare : *Glyphiulus bedosae* Golovatch, Geoffroy, Mauriès & VandenSpiegel, 2007; ∇ : *Glyphiulus houaphanhensis*, new species; \square : *Glyphiulus subbedosae* Likhitrakarn, Golovatch & Panha, 2017; \diamond : *Glyphiulus subcostulifer* Golovatch, Geoffroy, Mauriès & VandenSpiegel, 2007; \blacklozenge : *Glyphiulus percostulifer* Golovatch, Geoffroy, Mauriès & VandenSpiegel, 2007; \bullet : *Glyphiulus steineri*, new species.

Key to *Glyphiulus* species presently known to occur in Laos (Fig. 7), chiefly based on male characters, modified after Likhitrakarn et al. (2017)

1. Male leg 1 very strongly reduced, completely lacking any median structures.....2
- Male leg 1 either normal or reduced in size, but with a pair of paramedian coxal processes (Figs. 2B, C, 4C, D, 6C, D).....3
2. Paraprocts with a row of several strong setae near median marginal ridge; posterior gonopods broadly subquadrate, each half with a plumose apical flagellum (f).....*G. subbedosae*
- Paraprocts with a bare marginal ridge devoid of setae; posterior gonopods narrowly subrectangular.....*G. bedosae*
3. Carinotaxy formula of midbody rings $2+I/i+3/3+I/i+2$4
- Carinotaxy formula of midbody rings $2/2+I/i+3/3+I/i+2/2$ (Figs. 1D, E, 3D, E, 5D, E).....5

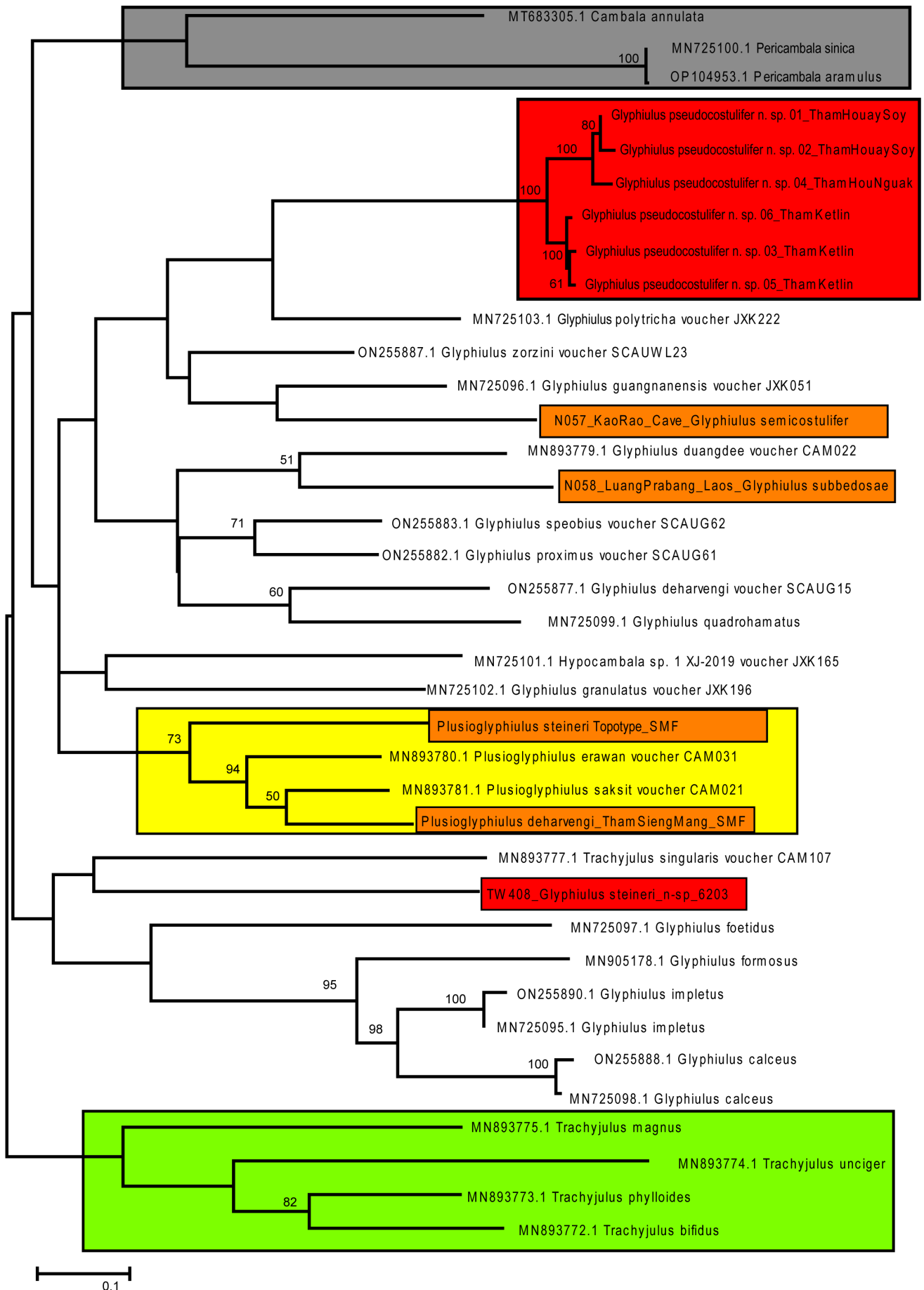


Figure 8. Maximum likelihood tree (ML) of millipedes in the family Cambalopsidae based on 671 bp of the COI gene. Clades of new species in this study are highlighted in red, newly sequenced species are highlighted in orange. Grey box = outgroup, green box = *Trachyjulus*, yellow box = *Plusioglyphiulus*. Numbers on nodes are bootstrap values (bs) from ML analysis, and are shown when >50%.

4. Carinotaxy formula of collum, I–VI+7a+pc+ma+pc+7a+VI–I, texture of both lateral-most crests micropunctate; male leg 1 with two low, paramedian, contiguous cones; each posterior gonopod with a long and bare flagellum..... *G. costulifer*
- Carinotaxy formula of collum, I+2c+III–VI+5c+6a+pc+ma+pc+6a+5c+VI–III+2c+I, both lateral-most crests smooth; male leg 1 with medially contiguous, apically diverging cones; each posterior gonopod with a long, distally plumose flagellum
..... *G. semicostulifer*
5. Ommatidia invisible or absent.....6
- Ommatidia present7
6. Colouration entirely pallid; adult body length 14–17 mm; carinotaxy formula of collum 1–4+5a+pc+ma; apicomesal processes (d) on the anterior gonopods broad and stout, apicolateral process (ap) being small and rounded; a distally plumose flagellum process (f) present on the posterior gonopods..... *G. percostulifer*
- Colouration usually brownish; adult body length 18.5–22.5 mm; carinotaxy formula of collum 1+2c+3–4+5c+6a+pc+ma (Fig. 5A–C); apicomesal processes (d) on the anterior gonopods long and slender (Fig. 6J, K), apicolateral process (ap) large, curved, and subdigitiform (Fig. 6H, I); a slim and smooth flagellum process (f) present on the posterior gonopods (Fig. 6J, K)
..... *G. houaphanhensis*, new species
7. Carinotaxic formula of collum: 1–2+3c+4a+5c+6+7c+8a+pc+ma; male leg 1 telopodites strongly reduced in size, 4-segmented; anterior gonopod with a subsecuriform coxosternum.....
..... *G. subcostulifer*
- Carinotaxic formula of collum: 1–5+6a+pc+ma (Figs. 1A, B; 3A, B); male leg 1 telopodites nearly normal, 5-segmented (Figs. 2B, C, 4C, D); anterior gonopod coxosternum with particularly high median outgrowths (Figs. 2H, I, 4H, I).....8
8. Carinotaxic formula of midbody rings: 2+I/i+3/3+I/i+2 (Fig. 1A, B, D, E, G, H); apicomesal processes (d) on the anterior gonopods longer and slender (Fig. 2H, I); without apicolateral process (ap) (Fig. 2H, I); tip of flagellum process (f) on the posterior gonopods pointed (Fig. 2J, K).....
..... *G. pseudocostulifer*, new species
- Carinotaxic formula of midbody rings: 2/2+I/i+3/3+I/i+2/2 (Fig. 3A, B, D, E, G, H); apicomesal processes (d) on the anterior gonopods broader and stout (Fig. 4H, I); with an evident, swollen, rounded apicolateral process (ap) (Fig. 4H, I); tip of flagellum process (f) on the posterior gonopods axeshaped (Fig. 4J, K) *G. steineri*, new species

Molecular barcoding analysis

For genetic analyses, we incorporated DNA sequences of the COI gene of our two new species, as well as two previously described *Glyphiulus* species from Laos and two species from the closely related genus *Plusioglyphiulus*, which were found in Cambodia. Interspecific genetic distances between *Glyphiulus* species and other members of the Cambalopsidae were high, with a minimum of 13.1% between *Glyphiulus impletus* Jiang, Guo, Chen & Xie, 2018 and *G. calceus* Jiang, Guo, Chen & Xie, 2018 with other *p*-distances in the family usually varying between 15–22% (Table 2).

The closest species to *Glyphiulus pseudocostulifer*, new species, in terms of genetic distance is *G. polytrichus* (Golovatch, Geoffroy, Mauriès & VandenSpiegel, 2011) (16.9%), which is also reflected in the phylogeny (Fig. 8), albeit without any statistical support. *Glyphiulus pseudocostulifer*, new species, was discovered in the caverns

of Ban Chom Ong, Oudomxay Province, situated in northern Laos. These caverns are approximately 560 kilometres away from the Yan Cave and the Cave Bi Ji Dong (Ca Wai), the type locality of *G. polytrichus* in Longzhou County, Guangxi Zhuang Autonomous Region, China. Consequently, a significant geographical divide exists between these two localities, in addition to distinct morphological differences.

The closest species to *Glyphiulus steineri*, new species, in terms of genetic distance is *G. guangnanensis* Jiang, Guo, Chen & Xie, 2018 (16.6%). However, this is not reflected in the phylogeny, where *G. steineri*, new species, groups with *Trachyulus singularis* (Attems, 1938), albeit without any statistical support (Fig. 8). Intraspecific distances could only be calculated from *G. pseudocostulifer*, new species, for which three populations could be sampled. The populations from Ban Houay Soy and Ban Chom Ong differ significantly by up to 6.9% (Table 2).

The high genetic distances in the COI gene between species is reflected in the phylogenetic tree (Fig. 8). Almost no grouping between species or even on the genus-level receives statistical support, but among the *Plusioglyphiulus* species, *P. erawan* Golovatch, Geoffroy, Mauriès & VandenSpiegel, 2011 is in a well-supported (94%) sister-group to *P. saksit* Golovatch, Geoffroy, Mauriès & VandenSpiegel, 2011 + *P. deharvengi* Golovatch, Geoffroy, Mauriès & VandenSpiegel, 2009 (Fig. 8).

DISCUSSION

In this study, three new species of the millipede genus *Glyphiulus* from Laos were described and fully illustrated based on specimens collected from caves located across various provinces of Laos. According to the revised classification created by Zhao et al. (2022), these three new species belong to the *sinensis*-group which are characterised by nearly fully developed and 5-segmented male first legs, as well as a pair of relatively large, unfused, and laterally extending paramedian coxal processes (Figs. 2B, D, 4D, E, 6D, E). In addition, we list two more distinct *Glyphiulus* species from Laos, currently only known from females, of which one occurs in direct sympatry with *G. houaphanhensis*, new species (Fig. 7).

According to the interspecific genetic distances, it was found that all four *Glyphiulus* species used in the study exhibit significantly high levels of genetic dissimilarity compared to other species (ranging from 14.9% to 27.1%, as indicated in Table 2). This result is consistent with the findings of Jiang et al. (2023) and Zhao et al. (2022), where values ranged between 13.08–24.68% and 17.2–27.1%, respectively. In the phylogenetic tree in Figure 8, the arrangement of *Glyphiulus* species displays probable resemblance to the phylogenetic tree proposed by Zhao et al. (2022), which delineates three species-groups. However, our phylogenetic tree (Fig. 8) lacks statistically adequate support because it was constructed from the mitochondrial COI gene alone.

In addition, the genera *Hypocambala*, *Plusioglyphiulus*, and *Glyphiulus* exhibited a polytomy. Reaching a definitive conclusion is challenging due to the utilisation of divergent COI regions, which indicate rapid evolution (Françoso et al., 2023). For example, Likhitrakarn et al. (2020) conducted an analysis using a longer 1,501 base pairs alignment dataset of the nuclear 28S rRNA and mitochondrial COI genes. Their analysis resulted in a robust clustering of *Glyphiulus* and other genera, but the number of analysed specimens was insufficient to conclusively determine the true relationships with clarity.

Additional research incorporating a broader range of genetic markers and comprehensive morphological analyses is necessary to enhance our understanding of the relationship between *Glyphiulus* and other closely related genera. For example, Jiang et al. (2021) conducted a comprehensive phylogenetic analysis utilising mitochondrial COI and 16S rRNA genes with two ribosomal nuclear genes. Their findings revealed distinct clades encompassing 26 *Glyphiulus* species, two *Plusioglyphiulus* species, and five *Trachyzulus* species. Their results provided a much better resolution of the relationship between *Glyphiulus* and *Plusioglyphiulus* species. Notably, the species *Hypocambala zizhongii* Jiang, Zhang, Chen & Xi, 2021 showed a clear separation from the remaining taxa and was grouped together with the outgroup.

The discovery of three new millipede species contributes significantly to expanding our knowledge of millipede diversity in Laos. The country has emerged as a hotspot for millipede diversity, with a substantial number of new species having been discovered in recent years. The remarkable biodiversity found in the Greater Mekong region, where Laos is situated, underscores the urgent need for ongoing efforts in biodiversity exploration and conservation. Despite the progress made, our understanding of the millipede fauna in Laos still remains incomplete, with only a small fraction of its diversity having been thoroughly examined. It is beyond doubt that as research advances on both surface-dwelling and cave-dwelling millipede populations in Laos, numerous additional discoveries will come to light. Even when focusing solely on the family Cambalopsidae, it becomes evident that we have merely begun to scratch the surface of the iceberg (Golovatch et al., 2007a).

ACKNOWLEDGEMENTS

We are very grateful to Claudia Etzbauer (ZFMK, Bonn) who extracted and processed the molecular samples. Many thanks to Peter Jäger and Julia Altmann (Senckenberg Museum Frankfurt) for being great hosts and loaning out their valuable material. Helmut Steiner and his caving team collected most of the samples analysed here, for which we are very grateful. Many thanks to the editor Wendy Wang, the reviewers Henrik Enghoff, Sergei I. Golovatch and two anonymous ones, whose numerous comments greatly improved our work.

LITERATURE CITED

- Altschul SF, Madden TL, Schäffer AA, Zhang J, Zhang Z, Miller W & Lipman DJ (1997) Gapped BLAST and PSI-BLAST: a new generation of protein database search programs. *Nucleic Acids Research*, 25(17): 3389–3402.
- Astrin JJ & Stüben PE (2008) Phylogeny in cryptic weevils: molecules, morphology and new genera of western Palaearctic Cryptorhynchinae (Coleoptera: Curculionidae). *Invertebrate Systematics*, 22(5): 503–522.
- AVMA (2020) AVMA guidelines for the euthanasia of animals. <https://www.avma.org/sites/default/files/2020-02/Guidelines-on-Euthanasia-2020.pdf> (Accessed 24 July 2023).
- Cook OF (1895) The Craspedosomatidae of North America. *Annals of the New York Academy of Sciences*, 9: 1–100.
- Enghoff H, Dohle W & Blower JG (1993) Anamorphosis in millipedes (Diplopoda) – the present state of knowledge with some developmental and phylogenetic considerations. *Zoological Journal of the Linnean Society*, 109: 103–234.
- Felsenstein J (1985) Phylogenies and the comparative method. *The American Naturalist*, 125(1): 1–15.
- Françoso E, Zuntini AR, Ricardo PC, Santos PKF, Araujo NS, Silva JPN, Gonçalves LT, Brito R, Gloag R, Taylor BA, Harpur BA, Oldroyd BP, Brown MJF & Arias MC (2023) Rapid evolution, rearrangements and whole mitogenome duplication in the Australian stingless bees *Tetragonula* (Hymenoptera: Apidae): A steppingstone towards understanding mitochondrial function and evolution. *International Journal of Biological Macromolecules*, 242(1): 124568.
- Gervais P (1847) Myriapodes. In: Walckenaer OA & Gervais P (eds) *Histoire naturelle des Insectes. Aptères IV*, 4: 1–623.
- Golovatch SI (2018) On several new or poorly-known Oriental Paradoxosomatidae (Diplopoda: Polydesmida), XXV. *Arthropoda Selecta*, 27(4): 261–277.
- Golovatch SI (2019) The millipede genus *Cryptocorypha* Attems, 1907 revisited, with descriptions of two new Oriental species (Diplopoda: Polydesmida: Pyrgodesmidae). *Arthropoda Selecta*, 28(2): 179–190.
- Golovatch SI, Geoffroy JJ, Mauriès JP & VandenSpiegel D (2007a) Review of the millipede genus *Glyphiulus* Gervais, 1847, with descriptions of new species from Southeast Asia (Diplopoda, Spirostreptida, Cambalopsidae). Part 1: the *granulatus*-group. *Zoosystema*, 29(1): 7–49.
- Golovatch SI, Geoffroy JJ, Mauriès JP & VandenSpiegel D (2007b) Review of the millipede genus *Glyphiulus* Gervais, 1847, with descriptions of new species from Southeast Asia (Diplopoda, Spirostreptida, Cambalopsidae). Part 2: the *javanicus*-group. *Zoosystema*, 29(3): 417–456.
- Golovatch SI, Geoffroy JJ, Mauriès JP & VandenSpiegel D (2009) Review of the millipede genus *Plusioglyphiulus* Silvestri, 1923, with descriptions of new species from Southeast Asia (Diplopoda, Spirostreptida, Cambalopsidae). *Zoosystema*, 31(1): 71–116.
- Golovatch SI, Geoffroy JJ, Mauriès JP & VandenSpiegel D (2011a) New species of the millipede genus *Glyphiulus* Gervais, 1847 from the *granulatus*-group (Diplopoda: Spirostreptida: Cambalopsidae). *Arthropoda Selecta*, 20(2): 65–114.
- Golovatch SI, Geoffroy JJ, Mauriès JP & VandenSpiegel D (2011b) New species of the millipede genus *Glyphiulus* Gervais, 1847 from the *javanicus*-group (Diplopoda: Spirostreptida: Cambalopsidae). *Arthropoda Selecta*, 20(3): 149–165.
- Golovatch SI & VandenSpiegel D (2017) One new and two little-known species of the millipede family Cryptodesmidae from Indochina (Diplopoda, Polydesmida). *Zoologicheskii Zhurnal*, 96(7): 757–767.

- Hall TA (1999). BioEdit: a user-friendly biological sequence alignment editor and analysis program for Windows 95/98/NT. *Nucleic Acids Symposium Series*, 41(41): 95–98.
- Hebert PD, Ratnasingham S & De Waard JR (2003) Barcoding animal life: cytochrome c oxidase subunit 1 divergences among closely related species. *Proceedings of the Royal Society of London. Series B: Biological Sciences*, 270: 96–99.
- Jiang XK, Guo X, Chen H & Xie Z (2018) Four new species of the *Glyphiulus javanicus* group (Diplopoda, Spirostreptida, Cambalopsidae) from Southern China. In: Stoev P & Edgecombe GD (eds) *Proceedings of the 17th International Congress of Myriapodology*, Krabi, Thailand. *ZooKeys*, 741: 155–179.
- Jiang XK, Lv JC, Guo X, Yu ZG & Chen HM (2017) Two new species of the millipede genus *Glyphiulus* Gervais, 1847 from Southwest China (Diplopoda: Spirostreptida: Cambalopsidae). *Zootaxa*, 4323(2): 197–208.
- Jiang XK, Shear WA, Ye LP, Chen HM & Xie ZC (2023) Recovery of the family status of Pericambalidae Silvestri, 1909, stat. nov. (Diplopoda: Spirostreptida: Cambalidea), with a revision of the genera and species from China. *Invertebrate Systematics*, 37(1): 78–100.
- Jiang XK, Zhang ZX, Chen HM & Xie ZC (2021) Description of *Hypocambala zizhongii* sp. nov. and the new combination, *Glyphiulus polytrichus* (Golovatch et al., 2011) comb. nov., based on morphological and molecular data (Spirostreptida: Cambalidea: Cambalopsidae). *Zootaxa*, 4903(3): 405–418.
- Likhitrakarn N, Golovatch SI, Inkhavilay K, Sutcharit C, Srisonchai R & Panha S (2017) Two new species of the millipede genus *Glyphiulus* Gervais, 1847 from Laos (Diplopoda, Spirostreptida, Cambalopsidae). *ZooKeys*, 722(3): 1–18.
- Likhitrakarn N, Golovatch SI & Jantarit S (2021) Two new species of the millipede genus *Glyphiulus* Gervais, 1847 (Diplopoda, Spirostreptida, Cambalopsidae) from caves in northern Thailand. *ZooKeys*, 1056: 173–189.
- Likhitrakarn N, Golovatch SI, Jeratthitikul E, Srisonchai R, Sutcharit C & Panha S (2020) A remarkable new species of the millipede genus *Trachyjulus* Peters, 1864 (Diplopoda, Spirostreptida, Cambalopsidae) from Thailand, based both on morphological and molecular evidence. *ZooKeys*, 925: 55–72.
- Likhitrakarn N, Golovatch SI & Panha S (2014) A checklist of the millipedes (Diplopoda) of Laos. *Zootaxa*, 3754(4): 473–482.
- Liu WX & Wynne JJ (2019) Cave millipede diversity with the description of six new species from Guangxi, China. *Subterranean Biology*, 30: 57–94.
- Nguyen AD, Sierwald P & Ware S (2023) First record of the genus *Touranella* Attems, 1937 (Diplopoda, Polydesmida, Paradoxosomatidae) from Laos, with a description of a new species. *ZooKeys*, 1145: 169–180.
- Peters WCH (1864) Übersicht der im Königl. zoologischen Museum befindlichen Myriopoden aus der Familie der Polydesmi, so wie Beschreibungen einer neuen Gattung, *Trachyjulus*, der Juli und neuer Arten der Gattung *Siphonophora*. *Monatsberichte der Königlich Preussischen Akademie der Wissenschaften zu Berlin*, 1864(7): 529–551.
- Sagorny C & Wesener T (2017). Two new giant pill-millipede species of the genus *Zoosphaerium* endemic to the Bemanevika area in northern Madagascar (Diplopoda, Sphaerotheriida, Arthrosphaeridae). *Zootaxa*, 4263(2): 273–294.
- Silvestri F (1897) Neue Diplopoden. *Abhandlungen und Berichte des Königl. Zoologischen und Anthropologisch-Ethnographischen Museums zu Dresden*, 6(9): 1–23.
- Silvestri F (1923) Descriptions of some Indian and Malayan Myriapoda Cambaloidea. *Records of the Indian Museum*, 25: 181–193.
- Srisonchai R, Inkhavilay K, Ngor PB, Sutcharit C & Likhitrakarn N (2023) Uncovering endemism in high montane forests: two new species of millipede genus *Tylopus* Jeekel, 1968 (Diplopoda: Polydesmida: Paradoxosomatidae) from Cambodia and Laos. *Tropical Natural History, Supplement 7*: 153–166.
- Tamura K & Nei M (1993) Estimation of the number of nucleotide substitutions in the control region of mitochondrial DNA in humans and chimpanzees. *Molecular Biology and Evolution*, 10(3): 512–526.
- Tamura K, Stecher G, Peterson D, Filipski A & Kumar S (2013) MEGA6: molecular evolutionary genetics analysis version 6.0. *Molecular Biology and Evolution*, 30(12): 2725–2729.
- Tavaré S (1986) Some probabilistic and statistical problems on the analysis of DNA sequence. *Lecture of Mathematics for Life Science*, 17: 57.
- Wesener T (2019) First records of giant pill-millipedes from Laos (Diplopoda, Sphaerotheriida, Zephroniidae). *Zootaxa*, 4563(2): 201–248.
- Wesener T, Moritz L & Akkari N (2023) Integrative redescription of the sucking millipede genus *Dawydoffia* Attems, 1953, with a description of a new species and a transfer to the family Hirudisomatidae (Diplopoda, Polyzoniida). *Zootaxa*, 5263(3): 411–429.
- WWF (2021) New Species Discoveries in the Greater Mekong 2020. https://files.worldwildlife.org/wwfmsprod/files/Publication/file/5s8a16akht_WWF_New_species_discoveries_2020_PAGES_final_compressed.pdf?_ga=2.48214626.451034281.1683627052-840442351.1683627052 (Accessed 4 May 2023).
- Zhao Y, Guo WR, Golovatch SI & Liu WX (2022) Revision of the *javanicus* species group of the millipede genus *Glyphiulus* Gervais, 1847, with descriptions of five new species from China (Diplopoda, Spirostreptida, Cambalopsidae). *ZooKeys*, 1108: 89–118.